

Topical Penetration of Piroxicam Is Dependent on the Distribution of the Local Cutaneous Vasculature

Nancy A. Monteiro-Riviere,^{1,4} Alfred O. Inman,¹
Jim E. Riviere,¹ Stephen C. McNeill,² and
Michael L. Francoeur^{2,3}

Received December 2, 1992; accepted March 16, 1993

The mechanism of the topical delivery of piroxicam, a nonsteroidal antiinflammatory drug, has been controversial as to whether systemic absorption is required for topical efficacy. This study, using *in vivo* pigs treated with topical ³H-piroxicam gel, was designed to assess the role of systemic absorption on its delivery to deep tissues. Further, the role of the structure of the cutaneous vasculature (e.g., direct cutaneous or musculocutaneous) was studied. Finally, piroxicam delivery was measured using *in vitro* diffusion cells with pig skin obtained from the same sites to determine inherent permeability independent of vascular anatomy. These studies showed that penetration of the radiolabel occurred in subcutaneous and muscle tissue only under the dosed sites and not at the remote sites, ruling out systemic absorption as a prerequisite for local delivery. Tissue penetration *in vivo* was enhanced at the musculocutaneous compared to the direct cutaneous sites. In contrast, *in vitro* flux was identical in skin harvested from the two vascular sites, suggesting that the vasculature plays a pivotal role in deep tissue penetration of piroxicam. In conclusion, local delivery of topical drugs occurs independent of systemic absorption and the nature of the cutaneous vasculature at different sites must be taken into consideration for optimal delivery.

KEY WORDS: piroxicam; pig skin; topical drug delivery; cutaneous vasculature; diffusion cells.

INTRODUCTION

Topical delivery of nonsteroidal antiinflammatory drugs directly to the site of localized distress pain is a desirable feature because local pain can be alleviated without adverse systemic side effects. However, there has been considerable debate as to whether the topical effect is due to direct penetration or is secondary to systemic absorption and recirculation. Previous studies in rats strongly implied that topical administration of piroxicam in male rats resulted in a high concentration of the drug in the underlying musculature. These concentrations could not be attributed solely to entry from the systemic circulation (1). Thus, cutaneous vasculature apparently does not function as an infinite sink that removes all topically applied drugs to the systemic circulation (2). Other investigators have alluded to this mechanism

of local topical drug delivery (3–5). In fact, it has been demonstrated that local modulation of the cutaneous vasculature by co-iontophoresis of vasoactive compounds could affect drug distribution to underlying tissues (6). Based upon these studies (1–6), we hypothesized that the local vasculature underlying the topical application site creates a convective force carrying topically applied drug down into the underlying tissues without being absorbed into the systemic circulation. To test this hypothesis, we utilized the Yorkshire pig, which is an accepted animal model for human skin. This model also has regions of the skin which are known to be differentially supplied with blood either by direct cutaneous or by musculocutaneous arteries. This allows one to study the effect of different patterns of the subcutaneous vasculature on topical drug penetration.

Piroxicam, 4-hydroxy-2-methyl-*N*-2-pyridinyl-2H-1,2-benzothiazine-3-carboxamide-1,1-dioxide, is a reasonably potent nonsteroidal antiinflammatory drug in which the dermal penetration was investigated *in vivo* (pigs) and *in vitro* (diffusion cells). The *in vivo* phase of the study had two objectives. First, the cutaneous disposition of topically applied piroxicam was studied both directly under the application site and at three remote locations. This enabled us to assess the role of systemic absorption on deep tissue delivery. Second, the topical penetration was assessed after delivery of piroxicam to two tissue beds, one that is vascularized by direct cutaneous arteries and the other that is vascularized by musculocutaneous arteries (Fig. 1). The *in vitro* diffusion cell model was used to assess passive delivery of piroxicam using pig skin obtained from the identical area of the pig used in the *in vivo* studies. Therefore, this study will determine the role of the cutaneous vasculature in the topical delivery of piroxicam to the subcutaneous structures.

MATERIALS AND METHODS

In Vivo

Eight weanling female Yorkshire pigs (*Sus scrofa*) weighing 40–60 lb were subjected to a complete physical examination, including urine, fecal, and blood analysis prior to experimentation to insure the proper health of the animals. Twenty-four hours prior to their use in an experiment, the left and right thoracic and inguinal regions were clipped of body hair. Pigs were immobilized with 2.5 mg/kg xylazine and 20 mg/kg ketamine and small additional dosages of each drug were given throughout the dosing in order to keep the animals under sedation. The pigs were placed in a dorsal recumbent position and four body sites were chosen. Areas A and C are perfused by cranial musculocutaneous arteries, and areas B and D by caudal direct cutaneous arteries (Fig. 1). The compound (100 mg of ³H-piroxicam gel) was applied to one site per pig. The ³H-piroxicam was formulated into a Carbopol-based gel where the final concentration of the drug was 0.5% (w/w).

Radiolabeled piroxicam (4-hydroxy-2-methyl-*N*-2-pyridinyl-2H-1,2-benzothiazine-3-carboxamide-1,1-dioxide) was obtained by tritium exchange (7). After repeated recrystallizations in ethanol, HPLC analysis demonstrated a purity of greater than 98%. The final specific activity of piroxicam

¹ North Carolina State University, Cutaneous Pharmacology and Toxicology Center, 4700 Hillsborough Street, Raleigh, North Carolina 27606.

² Pfizer, Inc., Central Research Division, Dermal Therapeutics, Groton, Connecticut 06340.

³ Current address: Pharmetrix Corporation, 1330 O'Brien Drive, Menlo Park, California 94025.

⁴ To whom correspondence should be addressed.

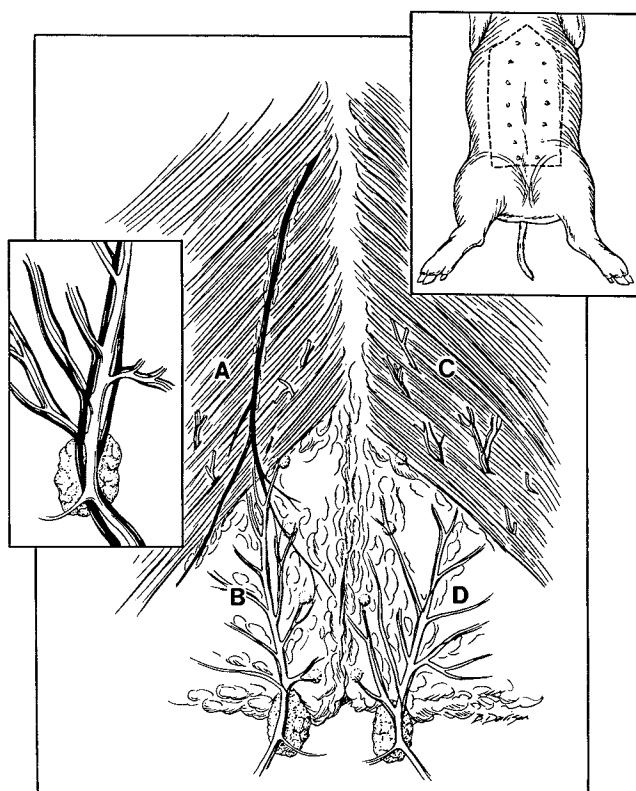


Fig. 1. Cutaneous vasculature of the ventral surface of the pig. Cranial sites A and C represent skin that is supplied by musculocutaneous arteries, while caudal sites B and D represent regions supplied by direct cutaneous arteries.

was found to be 27 $\mu\text{Ci}/\text{mg}$, and the tritium label was determined by mass spectroscopy and ^{13}C -NMR to be singly attached to the 8-position on the aromatic ring of benzothiazine nucleus (8). Previous animal studies in rats, dogs, and rhesus monkeys had found this tritium label to be relatively stable and useful in identifying specific metabolites of piroxicam (9).

The gel was weighed and applied quickly and evenly to a 10-cm² dose area. The excess gel was returned to the weighing paper and the final weight recorded. A rigid nonocclusive shield was placed over the dosing area and secured with cyanoacrylate and Elasticon tape. A shield was also secured over the nondosed remote sites. This was to prevent any cross-contamination between sites. A fiberglass screen was wrapped around the entire midriff of the pig and the edges were secured with Elasticon tape to cover all sites (A, B, C, and D). The dosing site was randomized so that each site was dosed twice over the course of the study.

After dosing, the pigs were allowed to recover from the anesthesia and then housed separately in stainless-steel metabolism chambers and monitored during the 12-hr exposure. This time point was selected based on preliminary isolated perfused porcine skin flap studies which showed piroxicam flux plateauing at 8 hr. Thus, tissue concentrations at 12 hr should reflect a postabsorptive equilibrium. Following exposure, the pigs were sedated with ketamine and xylazine. Then a 22-gauge butterfly catheter was inserted into the intermediate auricular vein and the patency of the catheter

tested with 2–4 mL of a 0.9% saline solution. The catheter was secured to the ear with adhesive tape and sodium pentobarbital (65 mg/mL) was administered intravenously at 26 mg/kg of body mass. The screen and shields from the three nondosed sites and piroxicam-dosed site were removed and the dosing site was swabbed lightly with two 2 \times 2-in. gauze pads containing 1 mL of a soapy wash solution. Each of the pads was placed in a separate scintillation vial containing 15 mL of ethanol. The area was blotted dry with a gauze pad and placed in a vial containing 15 mL of ethanol. The area was tape-stripped 12 times, with each two successive strips placed in a scintillation vial containing 15 mL of ethyl acetate.

The three nondosed areas were dissected to the peritoneum (approximately 18 mm in depth for the cranial and 9 mm for the caudal sites) and weighed. Two longitudinal cores 1 cm² were trimmed from each site and weighed. One core was embedded in OCT compound, quenched in an isopentane well cooled by liquid nitrogen, and immediately stored at -80°C . The remaining core was divided through the subcutaneous layer, and each portion weighed and placed in separate scintillation vials containing 15 mL of Soluene 350 (Hewlett-Packard Co., Inc.). Additional time-course studies showed that piroxicam did not evaporate out of the Soluene. Tissue, dissected from an area adjacent to the frozen core to maintain anatomical congruity, was weighed and fixed in 10% neutral buffered formalin for histologic evaluation. Upon completion of sampling, the pig was euthanized with an intravenous injection of Beuthanasia-D (Shering-Plough).

The OCT embedded tissue core ($n = 4$ per pig) was mounted in a cryostat and allowed to equilibrate to the chamber temperature (approximately -30°C). The microtome section thickness was set to 60 μm and the block carefully faced until a complete section was obtained. All partially faced sections were placed in a combustocone at -30°C , followed by two successive sections per cup until no tissue remained. The top and bottom of the knife, the section shield, and the tissue forceps were thoroughly cleaned with a dry Kimwipe following each two sections. The sectioned tissue was stored at -30°C until combusted to prevent piroxicam volatilization. All swabs, tape strips, and solubilized tissue were aliquoted into cups with pads. The samples were oxidized and the resulting tritium content assayed.

Samples for light microscopy (LM) were fixed in 10% neutral buffered formalin, routinely processed, infiltrated with paraffin in an automated tissue processor (Tissue Tek VIP 1000, Miles Laboratories, Inc., Naperville, IL.), and then embedded in an embedding station (Tissue Tek, Miles Laboratories). Six-micron sections were cut on a rotary microtome (Reichert-Jung 820), stained with hematoxylin and eosin (Histomatic Code-On Stainer, Fisher Scientific), and coverslipped with Permount for histologic evaluation.

Data were analyzed using VMS SAS (Version 6.06) software. The net radioactivity for each cup was calculated by subtracting the mean background activity (disintegrations per minute; dpm) from the raw dpm and extrapolating to the area of the entire dose site. The net dpm per section was calculated by adjusting for the number of sections per cup. The data were smoothed using a Lagrange interpolation of 1^o and plotted as absolute dpm and as percentage of applied dose activity (mean \pm SE; $n = 4$ pigs per group) versus

Table I. *In Vivo* Absorption of Piroxicam in Cranial and Caudal Sites (Mean \pm SE)

Sites	Cumulative mass (mg) ^a	Mean penetration depth (μ m)	% applied compound ^b
Cranial	8.36 \pm 2.00	1742.70 \pm 353.51	0.00430 \pm 0.00140
Caudal	2.69 \pm 0.51	1214.66 \pm 103.98	0.00018 \pm 0.000062

^a Estimated from the AUC of the penetration profile at the depth of 9480 μ m.

^b Discrete compound values estimated at 9480 μ m.

tissue depth. Statistical analysis was performed using a GLM procedure [*T* tests (LSD) and Tukey's studentized range (HSD) test] for section mean (absolute and normalized) dpm at each 60- μ m depth.

In Vitro Diffusion Cells

Freshly excised dermatomed pig skin (400- μ m) samples taken from cranial and caudal sites from additional pigs were mounted in standard Franz diffusion cells with an exposed surface area of 3 cm². To initiate each experiment, the gel was applied as a thin film (10 mg/cm²) to the stratum corneum surface. For the indicated surface area, the total dose of piroxicam applied was 150 μ g. The receiver compartment contained 5 mL of phosphate-buffered saline (pH 7.4), which was completely removed and replaced at each sampling time point (2, 4, 6, 8, 12, 24, and 48 hr). The resulting solutions were analyzed with conventional liquid scintillation tech-

niques, counting triplicate aliquots from each sample for 10 min on a Packard 2000 CA liquid scintillation analyzer (Packard Instruments, Sterling, VA), which corrected for quenching and chemiluminescence. Blank and spiked buffered Soluene 350 were processed in parallel as standard controls. Statistical analysis was performed using the Student's *t* test.

RESULTS

In Vivo

The passive *in vivo* penetration of piroxicam was variable, with a higher penetration in the cranial sites compared to the caudal sites. This was illustrated by a higher cumulative compound mass and mean penetration depth (MPD) in the cranial sites (Table I). Figure 2 compares the absolute mean penetration profiles of piroxicam for cranial and caudal sites. Normalization of the data by the activity of the topically applied compound had little effect on the penetration profile (Fig. 3). The distribution of the compound within dose sites is summarized in Table II.

All nondosed sites were assayed for ³H-piroxicam using the frozen serial sections and the solubilized tissue cores. Radioactivity only slightly above normal background levels was noted at discrete depths, indicating minimal compound crossover from the dosed site.

Statistical analyses were performed on absolute and normalized activity profiles as outlined in Table III. Briefly, a significant difference ($P < 0.05$) was found between area penetration profiles in the absolute and normalized applied activity at most depths from 900 to 9480 μ m. Using LM,

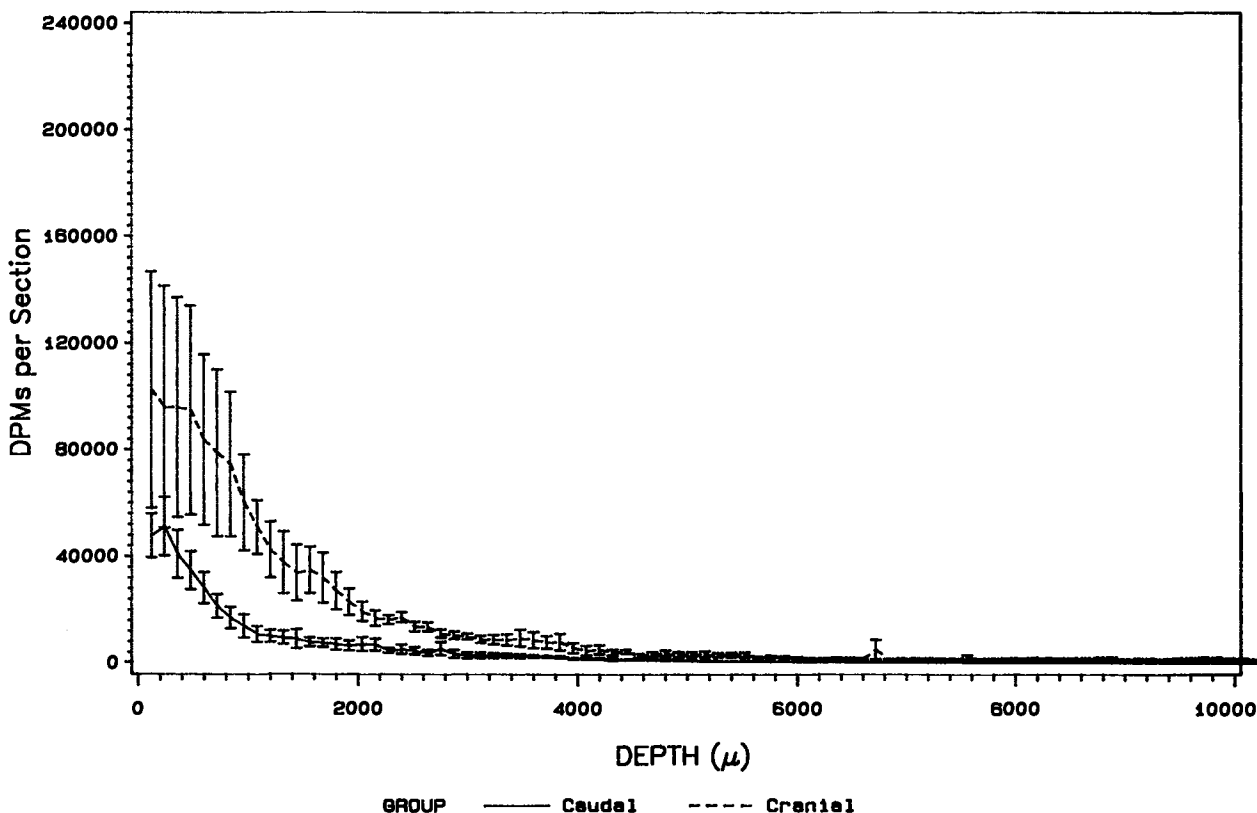


Fig. 2. The absolute mean penetration profiles of ³H-piroxicam versus depth from the cranial and caudal skin dosing sites ($n = 8$).

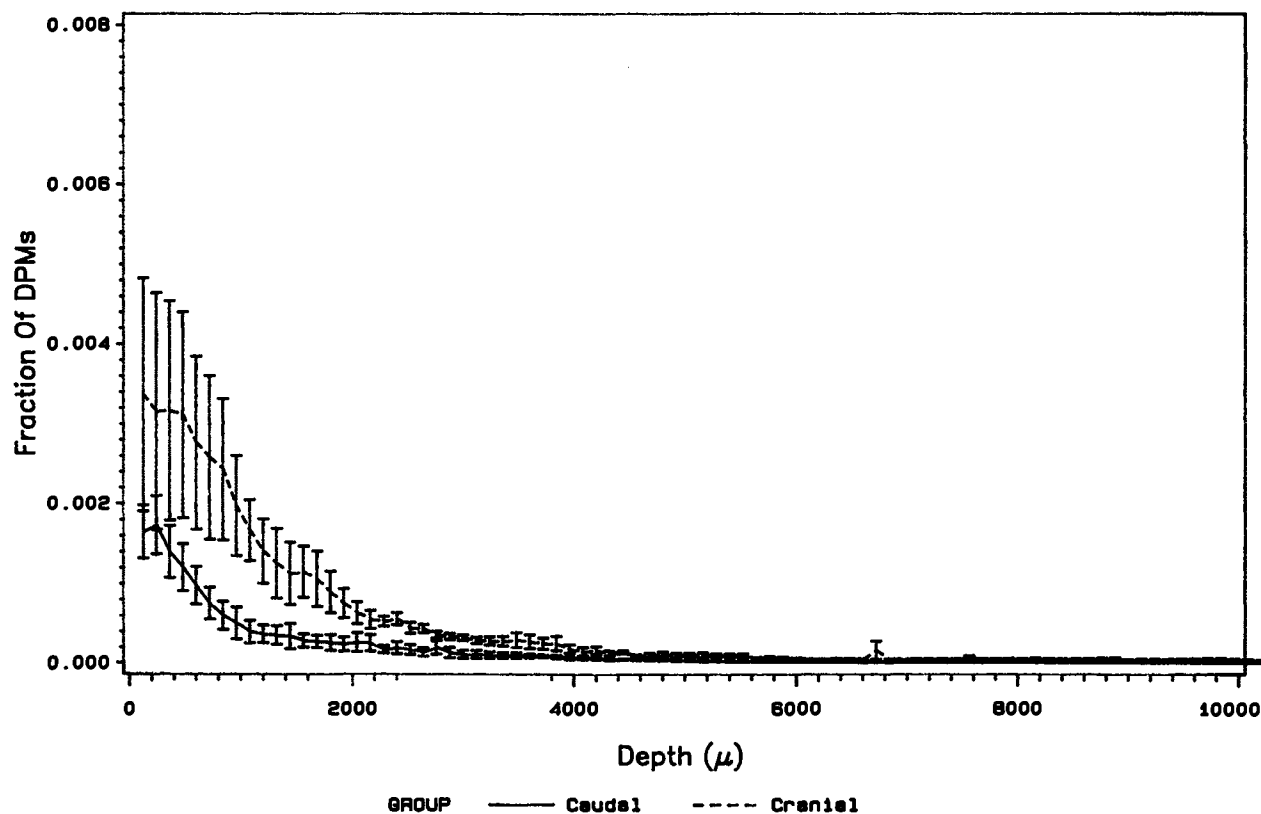


Fig. 3. Percentage of applied dose of ^3H -piroxicam as a function of depth from cranial and caudal skin dosing sites ($n = 8$).

these depths correlated to microscopic structures found in the deeper dermis (e.g., hair follicles, apocrine sweat glands), the subcutaneous layer (e.g., adipose tissue, blood vessels, nerves), and the skeletal muscle layers (Table IV). In the normalized absorbed activity profiles, however, significant differences ($P < 0.05$) between the cranial and the caudal areas were found at more discrete depths.

Analysis of variance was performed using T tests (LSD) and Tukey's studentized range (HSD) test on the variables listed in Table I. The analysis shows significant differences ($P < 0.05$) between the cranial and the caudal sites in the mean cumulative mass, the percentage of applied compound, and the percentage of absorbed compound.

In Vitro Diffusion Cells

The *in vitro* permeability studies indicated that there was no statistically significant ($P < 0.01$) difference in the permeability of skin harvested from either the cranial or the caudal areas to piroxicam (Table V).

DISCUSSION

The results of this study indicate that topical penetration of piroxicam is not dependent upon absorption into the systemic circulation, since only background concentrations of piroxicam were detected at the nondosed, remote sites. Further, optimal penetration to deeper structures is dependent

Table II. *In Vivo* Distribution of Piroxicam (%) in Cranial and Caudal Dose Sites

Sites	Pig No.	Site	Swab	Tape strip	Dose site		Whole site	Recovery
					Skin ^a	Fat & muscle ^b		
Cranial	1	C	39.1	1.7	2.2	1.1	3.4	44.1
	4	A	54.2	3.5	11.1	1.3	12.4	70.1
	5	C	58.6	2.6	12.8	0.4	13.2	74.4
	7	A	69.6	3.0	5.0	1.4	6.4	79.0
Caudal	2	B	61.2	0.6	1.5	0.1	1.6	63.5
	3	D	62.9	1.3	2.5	0.1	2.6	66.9
	6	D	62.0	2.0	5.2	0.3	5.5	69.5
	8	B	68.9	1.7	1.8	0.1	1.9	72.5

^a Includes stratum corneum, epidermis, dermis, and subcutaneous fat down to a depth of 3600 μm .

^b Includes subcutaneous fat and muscle beyond a depth of 3600 μm .

Table III. Depth at Which Significant Differences ($P < 0.05$) Exist Between the Cranial and the Caudal Sites: Comparison of Absolute and Percentage of Applied Dose Absorbed

Absolute activity depth (μm) ^a	Percentage of applied dose depth (μm) ^b
900–1200	1020–1200
1500–2640	1500–1560
	1860–1920
	2220–2640
2820–3360	2820–3120
4380–4440	4380–4440
5220–5400	5220–5400
5580–6600	5580–6600
6780–7320	6780–7320
7620–8640	7620–8640
9060–9480	9060–9480

^a See Fig. 2 for profile.

^b See Fig. 3 for profile.

upon the anatomical configuration of the cutaneous vasculature. In these studies tritium radioactivity was assayed to reflect piroxicam disposition. Based on previous analytical chemistry and metabolism studies using ³H-piroxicam (8,9), we believe that this is a valid assumption.

Penetrating musculocutaneous vessels appears to be needed to provide a conduit for the penetration of drug to the subdermal levels. The lack of differences in extent and rates of penetration in the *in vitro* diffusion study using skin from these same sites rules out skin permeability differences as being the cause of enhanced tissue delivery beneath the cranial site. Therefore, a constant fraction of piroxicam is absorbed across the stratum corneum/epidermal barrier. In the site perfused by direct cutaneous vasculature, most of this absorbed drug enters the systemic blood and is eliminated from the animal. In contrast, the site perfused by musculocutaneous arteries retained a larger fraction of the absorbed drug within deeper tissues perfused by the musculocutaneous vessels, resulting in a smaller fraction of the absorbed dose being available to the systemic circulation.

These findings have a significant impact on the utilization of simple *in vitro* systems and physicochemical models based on stratum corneum penetration to predict topical drug penetration. These approaches are extremely useful to determine the rate and extent of topical drug penetration across the stratum corneum and epidermis into the dermal tissue. However, the fraction of this "dermally deposited" drug subsequently absorbed into the systemic circulation is dependent upon both the physiology and the anatomy of the dermal microcirculation. The present work suggests that the

Table IV. Depth Correlation with Cutaneous Structure

Approximate depth (μm)	Microanatomy
0–15	Stratum corneum ^a
16–45	Epidermis
46–1749	Dermis
1750–4850	Subcutaneous layer
4851–10000	Muscle layers

^a Stratum corneum may be slightly thinner due to tape-stripping.

Table V. *In Vitro* Absorption of Piroxicam Using Diffusion Cells in Cranial and Caudal Sites (Mean \pm SE)^a

Sites	Flux (0–12 hr) ($\mu\text{g}/\text{cm}^2/\text{hr}$)	Cumulative amount transported ($\mu\text{g}/24$ hr)
Cranial	0.0062 \pm 0.0009	0.4100 \pm 0.0500
Caudal	0.0068 \pm 0.0003	0.4400 \pm 0.0800

^a $n = 7$ replicates.

penetrating musculocutaneous vasculature functions as a "convective" force driving the absorbed drug to deeper tissue beds. Drug in these vessels is not absorbed into the systemic circulation but, rather, distributed into the deeper tissues on the way to the systemic circulation. Significant differences exist in the magnitude of cutaneous blood flow at different sites within species and at the same sites between species (10). These differences reflect a vascular phenomenon that may also impact on local drug delivery.

The function of the cutaneous vasculature is important in predicting *in vivo* delivery of drugs administered topically by iontophoresis (6,11). In these cases, cutaneous depot formation was favored (and transdermal flux decreased) by co-iontophoresing with a vasoconstrictor drug. In contrast, the use of a vasodilator minimized the cutaneous depot (increased transdermal flux). Further modeling (12,13) suggests that the primary role of the cutaneous microcirculation is to change the volume of dermal tissue being perfused by modulating blood perfusion through nonexchanging shunts versus capillary beds which actually perfuse the tissue. These events could allow perfusion of deeper tissue beds which would promote the movement of topically applied drugs to these tissues. Thus, knowledge of the function and structure of the cutaneous microcirculation is essential to predict topical drug delivery accurately.

Structural differences exist between the skin of domestic and that of laboratory animals. Also, the thickness of the epidermis and dermis between species and within the same species in various regions of the body are different (10). Therefore, it is important to study skin permeability using skin from a species that closely resembles that of man. Pig skin resembles human skin in both structure and function. Pig and human skin are similar in having a sparse hair coat, a relatively thick epidermis, and a similar epidermal turnover kinetics, lipid composition, enzyme histochemistry, and carbohydrate biochemistry (14–16). Additionally, these studies are relevant because humans and pigs are of comparable body mass in contrast to smaller rodents. Therefore, the ratio of the topical dosing site area to the total body mass for a local application is similar in pigs and in humans. In rodents, this ratio represents a significant portion of skin surface area which in itself should result in significant systemic absorption.

Only a few authors have suggested that true deep local penetration exists following topical application of antiinflammatory drugs. Topical application of 1% indomethacin to inflamed paws of male rats resulted in a higher concentration of the drug in the exudate and muscle of the treated paw than the contralateral paw or blood (3). The efficacy of a topical application of a 1% piroxicam cream versus a single oral dose of 20 mg was studied in humans after exposure to ul-

traviolet-induced erythema giving rise to localized superficial inflammation. The topical application, in addition to showing greater efficacy, also showed a higher concentration of the drug in the underlying tissues than that was achieved with oral administration (4). Studies in male rats given piroxicam topically versus intravenously also showed that muscles underlying the dosing site had higher concentrations than did distant muscles after topical dosing. Also, these concentrations were greater than after intravenous administration (1).

In conclusion, these studies show that topical application of piroxicam can result in local delivery to deeper tissues without first being absorbed into the systemic circulation. Further, it would be expected that local application would be more efficacious at skin sites perfused by penetrating musculocutaneous vessels.

ACKNOWLEDGMENTS

The authors would like to thank Ms. Elise Cash for her technical assistance. This work was presented at the 1992 meeting of the American Association of Pharmaceutical Scientists in San Antonio, Texas.

REFERENCES

1. S. C. McNeill, R. O. Potts, and M. L. Francoeur. Local enhanced topical delivery of drugs: Does it truly exist? *Pharm. Res.* (in press).
2. J. E. Riviere and P. L. Williams. Pharmacokinetic implications of changing blood flow in skin. *J. Pharm. Sci.* 81:601-602 (1992).
3. Y. Wada, Y. Etoh, A. Ohira, H. Kimata, T. Koide, H. Ishihama, and Y. Mizushima. Percutaneous absorption and anti-inflammatory activity of indomethacin in ointment. *J. Pharm. Pharmacol.* 34:467-468 (1982).
4. J. Torrent, I. Izquierdo, M. J. Barbanoj, J. Moreno, J. Lauroba, and F. Jane. Anti-inflammatory activity of piroxicam after oral and topical administration on an ultraviolet-induced erythema model in man. *Curr. Ther. Res.* 44:340-347 (1988).
5. R. H. Guy and H. I. Maibach. Drug delivery to local subcutaneous structures following topical administration. *J. Pharm. Sci.* 72:1375-1380 (1983).
6. J. E. Riviere, N. A. Monteiro-Riviere, and A. O. Inman. Determination of lidocaine concentrations in skin after transdermal iontophoresis: Effects of vasoactive drugs. *Pharm. Sci.* 9:211-214 (1992).
7. T. R. Bosin and R. B. Rogers. Site specific deuteration or triation of benzothiophene and 1-methyl indole analogs of biologically-active indole derivatives. *J. Label. Compd.* 9:395-403 (1973).
8. E. B. Whipple. On the assignment of ^{13}C resonances in unsymmetrical orthodisubstituted benzene rings. *Org. Magn. Reson.* 10:23-25 (1977).
9. D. C. Hobbs and T. M. Twomey. Metabolism of piroxicam by laboratory animals. *Drug Metab. Dispos.* 9:211-214 (1992).
10. N. A. Monteiro-Riviere, D. G. Bristol, T. O. Manning, and J. E. Riviere. Interspecies and interregional analysis of the comparative histological thickness and laser Doppler blood flow measurements at five cutaneous sites in nine species. *J. Invest. Dermatol.* 95:582-586 (1990).
11. J. E. Riviere, B. Sage, and P. L. Williams. Effects of vasoactive drugs on transdermal lidocaine iontophoresis. *J. Pharm. Sci.* 80:615-620 (1992).
12. J. E. Riviere and P. L. Williams. Pharmacokinetic implications of changing blood flow in skin. *J. Pharm. Sci.* 81:601-602 (1992).
13. P. L. Williams and J. E. Riviere. A model describing transdermal iontophoresis delivery of lidocaine incorporating consideration of cutaneous microvasculature state. *J. Pharm. Sci.* (in press).
14. N. A. Monteiro-Riviere and M. W. Stromberg. Ultrastructure of the domestic pig (*Sus scrofa*) from one through fourteen weeks of age. *Anat. Histol. Embryol.* 14:97-115 (1985).
15. N. A. Monteiro-Riviere. Specialized technique: Isolated perfused porcine skin flap. In B. W. Kemppainen and W. G. Reif-enrath (eds.), *Methods for Skin Absorption*, CRC Press, Boca Raton, FL, 1990, pp. 175-189.
16. N. A. Monteiro-Riviere. Comparative anatomy, physiology, and biochemistry of mammalian skin. In D. W. Hobson (ed.), *Dermal and Ocular Toxicology: Fundamentals and Methods*, CRC Press, Boca Raton, FL, 1991, Chap. 1, pp. 3-71.